Elastic electron deuteron scattering with consistent meson exchange and relativistic contributions of leading order[*]

Hartmuth Arenhövel, Frank Ritz and Thomas Wilbois[†]

Institut für Kernphysik, Johannes Gutenberg-Universität, D-55099 Mainz, Germany

(February 9, 2008)

The influence of relativistic contributions to elastic electron deuteron scattering is studied systematically at low and intermediate momentum transfers ($Q^2 \leq 30$ fm^{-2}). In a (p/M)-expansion, all leading order relativistic π-exchange contributions consistent with the Bonn OBEPQ models are included. In addition, static heavy meson exchange currents including boost terms and lowest order $\rho\pi\gamma$-currents are considered. Sizeable effects from the various relativistic two-body contributions, mainly from π-exchange, have been found in form factors, structure functions and the tensor polarization T_{20}. Furthermore, static properties, viz. magnetic dipole and charge quadrupole moments and the mean square charge radius are evaluated.

PACS numbers: 13.40.Gp, 13.60.Fz, 21.45.+v, 25.30.Bf

I. INTRODUCTION

Recently, we had studied systematically for photo- and electrodisintegration of the deuteron the influence of relativistic contributions of leading order in a p/M-expansion [1,2]. In order to have a consistent framework of all one- and two-body current and boost contributions, we had chosen as interaction model the various Bonn OBEPQ versions [3,4]. In particular, we were interested in the role of heavy meson exchange. As general result we found that in electrodisintegration the ρ meson gives the most important heavy meson contribution whereas the influence of η, ω, σ, δ, and $(\rho/\omega)\pi\gamma$ is much smaller, in some observables completely negligible, in particular, near the quasifree kinematics. These findings were also valid for photodisintegration with some modifications, for example, in contrast to electrodisintegration the boost effects were almost negligible in photodisintegration for the energies considered because of the much smaller momentum transfers involved.

As a further step in these investigations it is naturally to study elastic electron scattering off the deuteron. On the one hand one would expect larger interaction effects, because also the nucleons in the final state are always off-shell, on the other hand, the leading order nonrelativistic meson exchange currents (MEC) from pion exchange will be absent due to their isovector character. Thus relativistic contributions to the MEC are expected to be more important. For this reason it appears mandatory to include all leading order relativistic contributions from pion exchange to one- and two-body charge and current densities including also wave function boost terms in a consistent framework. This is the main motivation for the present work in which we have used the same theoretical approach than in our previous investigations of deuteron photo- and electrodisintegration for the evaluation of the invariant form factors for elastic electron deuteron scattering.

Quite a few studies of this process exist in the literature which can be divided into two classes: (i) nonrelativistic approaches with relativistic contributions of leading order included, and (ii) covariant approaches. For a review of the status of the latter approaches see, e.g., more recent surveys in [5,6] and references therein. Furthermore, we would like to mention the most recent work by Phillips *et al.* [7] using a genuine three-dimensional relativistic framework. With respect to the first class of approaches, very few have adopted a consistent framework. Early developments may be found in [8] and in the reviews [9,10]. More recently, relativistic two-body currents from static pion and heavy meson exchange have been studied in [11–18]. Mosconi and Ricci [11] have studied the dependence of $A(Q^2)$ on the parametrization of the elementary nucleon form factors in the region $Q^2 \leq 20$ fm^{-2}. Their calculation is based on the Paris potential, and as current contributions they have included leading order relativistic one-body terms with boost, π- and ρ-exchange and $\rho\pi\gamma$-current, but no other heavier mesons. Within a quark model approach for the NN-interaction and the MEC, Buchman *et al.* [12] have studied this process with inclusion of leading order relativistic contributions to the currents, but without boost of the wave functions. Schiavilla and Riska [13] have calculated form factors and observables using a current operator constructed consistently with the Argonne v_{14} potential including

relativistic contributions, but again boost contributions have been left out completely. The same approach has been used by Wiringa *et al.* [16] for the newly developed charge-independence breaking Argonne v_{18} potential. In this work also static properties of the deuteron are reported. Within a pure one-pion-exchange model, the role of unitary equivalence of relativistic contributions to the charge density operator has been studied by Adam *et al.* [15] using a consistent approach for all leading order contributions to the charge density operator including boost terms. Essentially the same approach but using the realistic Paris and Bonn OBEPQ-B potentials has been applied to the charge and quadrupole form factors by Henning *et al.* [17], but the magnetic form factor has not been considered. Plessas *et al.* [18] have studied the influence of different parametrizations of the nucleon form factors on the observables. For the realistic Nijmegen and various Bonn potential models, they have included the pion pair and retardation currents, the usual relativistic one-body currents, and probably also the one-body boost. But the contributions from heavier meson exchange have been left out except for the $\rho\pi\gamma$-current.

The most extensive treatment of all leading order terms including boost has been presented by Tamura *et al.* [14] for elastic and inelastic electron deuteron scattering based on a one-boson-exchange (OBE) model for the NN-interaction which they had constructed specifically for this purpose and it is difficult to assess the general quality of this potential. In addition, they have also considered as a realistic NN-potential the Paris potential. Since this is a phenomenological potential and not a genuine OBE-potential, they had taken empirical values for meson-nucleon coupling constants and cut-off parameters. In view of the fact, that probably their OBEP has not reached the sophistication of the realistic Bonn OBEPQ models, the present work appears appropriate and justified in evaluating elastic electron deuteron scattering within a consistent approach based on a realistic genuine OBE-potential.

In the next section we will give a brief review of the relevant formalism for elastic electron deuteron scattering where the definition of form factors and structure functions are given. In Section III we first will sketch shortly the calculational framework on which our evaluation is based. Then the results on static electromagnetic properties, on form factors and structure functions will be presented and discussed.

II. BRIEF REVIEW OF FORMALISM

We will start with the general expression for elastic electron scattering cross section off a deuteron in the laboratory system in the one-photon-exchange approximation for unpolarized beam and target

$$\frac{d\sigma^{lab}}{d\Omega_e^{lab}} = \sigma_{Mott}^{lab}\left[(1+\eta)^{-2}\frac{\vec{q}_{lab}^{\,2}}{\vec{q}_c^{\,2}}W_L^{(c)}(Q^2) + \left(\frac{1}{2}(1+\eta)^{-1} + \tan^2\frac{\theta_e^{lab}}{2}\right)W_T^{(c)}(Q^2)\right], \tag{1}$$

where

$$\sigma_{Mott}^{lab} = \frac{\alpha^2\,\cos^2\frac{\theta_e^{lab}}{2}}{4\sin^4\frac{\theta_e^{lab}}{2}}\frac{k'_{lab}}{k_{lab}^3} \tag{2}$$

denotes the Mott cross section in the laboratory system with initial and final electron four momenta k_μ and k'_μ, respectively, α the fine structure constant, and the Lorentz scalar η is given by

$$\eta = \frac{Q^2}{4M_d^2}\,. \tag{3}$$

Here we have defined $Q^2 = -q_\mu^2$, where $q_\mu = k_\mu - k'_\mu = (\omega,\vec{q})$ denotes the four momentum transfer with $q_\mu^2 < 0$ and M_d the deuteron mass. We further note the following relations, expressing the lab energy and three-momentum transfers by η,

$$\vec{q}_{lab}^{\,2} = 4M_d^2\eta(1+\eta)\,, \qquad q_{0,\,lab} = 2M_d\,\eta\,. \tag{4}$$

The longitudinal and transverse structure functions $W_L^{(c)}$ and $W_T^{(c)}$, respectively, are related to the deuteron current matrix elements by

$$W_L^{(c)}(Q^2) = \frac{1}{12M_d^2}\sum_{m'm}|\langle d'm'|J_0(0)|d\,m\rangle^{(c)}|^2\,, \tag{5}$$

$$W_T^{(c)}(Q^2) = \frac{1}{12M_d^2}\sum_{\lambda=\pm1}\sum_{m'm}|\langle d'm'|J_\lambda(0)|d\,m\rangle^{(c)}|^2\,, \tag{6}$$

where d and d' denote the four momenta of initial and final deuteron states which are covariantly normalized as

$$\langle d'm'|dm\rangle = (2\pi)^3 2E_d \delta_{m'm}\delta(\vec{d}' - \vec{d})\,, \tag{7}$$

where $E_d = \sqrt{M_d^2 + \vec{d}^2}$. Here, $J_{\pm 1}$ denote the components of the current density operator transverse to the momentum transfer $\vec{q}$, and J_0 the following combination of charge density and longitudinal current density component

$$J_0 = -\frac{|\vec{q}|^2}{q_\mu^2}\left(\rho - \frac{\omega}{|\vec{q}|^2}\vec{q}\cdot\vec{J}\right) = \rho - \frac{\omega}{q_\mu^2}(\omega\rho - \vec{q}\cdot\vec{J})\,, \tag{8}$$

which reduces to the charge density ρ for a conserved current.

The superscript "(c)" in (5) and (6) indicates that the matrix elements and thus the structure functions in (1) are evaluated in a frame of reference "c" collinear to $\vec{q}$. Usually one chooses either the laboratory, the Breit or the antilab system. While $W_T^{(c)}(Q^2)$ is invariant for boosts collinear to the momentum transfer, the boost transformation of $W_L^{(c)}(Q^2)$ from the system "c" to the lab system is taken care of in (1) by the factor $\vec{q}_{lab}^2/\vec{q}_c^2$. Here, $\vec{q}_c$ denotes the three-momentum transfer in the c-system. The boost property of $W_L^{(c)}$ arises from the fact that $\frac{J_0}{|\vec{q}|}$ is invariant under collinear boosts. We note in passing that for elastic scattering the lab and antilab systems are equivalent for the evaluation since in this case one has $\vec{q}_{lab} = \vec{q}_{antilab}$.

Now we switch to noncovariant normalization and eliminate the c.m. motion by introducing the internal deuteron rest frame wave function $|1m\rangle$ writing

$$|d\,m\rangle = \sqrt{2E_d}\,|\vec{d}\rangle U(\vec{d})|1\,m\rangle\,. \tag{9}$$

Furthermore, $|\vec{d}\rangle$ denotes the plane wave of the c.m. motion and $U(\vec{d})$ the unitary operator of the boost from the deuteron rest system to the moving frame. The current matrix element is then reduced to the evaluation of the Fourier component $\tilde{J}_\lambda$ of the current density including boost contributions between intrinsic deuteron states

$$\langle d'm'|J_\lambda(0)|d\,m\rangle = 2\sqrt{E_{d'}E_d}\langle 1\,m'|\tilde{J}_\lambda(\vec{q})|1\,m\rangle\,, \tag{10}$$

where

$$\tilde{J}_\lambda(\vec{q},\,\vec{P}) = \int d^3R\, U^\dagger(\vec{d}')J_\lambda(0)\, U(\vec{d})e^{-i\vec{q}\cdot\vec{R}}\,, \tag{11}$$

with $\vec{q} = \vec{d}' - \vec{d}$ and $\vec{P} = \vec{d}' + \vec{d}$. For frames collinear to $\vec{q}$, $\vec{P}$ will be proportional to $\vec{q}$. Since such frames will be considered exclusively, we can drop $\vec{P}$ as an argument in $\tilde{J}_\lambda$. Introducing the multipole decomposition

$$\langle 1\,m'|\tilde{J}_\lambda(\vec{q})|1\,m\rangle = (-)^\lambda\sqrt{2\pi(1 + \delta_{\lambda 0})}$$
$$\sum_{LM}i^L\hat{L}\langle 1\,m'|\left(\delta_{\lambda 0}C_{LM} + \delta_{|\lambda|1}(T_{LM}^{(e)} + \lambda\,T_{LM}^{(m)})\right)|1\,m\rangle\,, \tag{12}$$

one defines the invariant charge monopole and quadrupole, and magnetic dipole form factors $G_C^{(c)}(Q^2)$, $G_Q^{(c)}(Q^2)$, and $G_M^{(c)}(Q^2)$, respectively, in terms of the reduced matrix elements of the corresponding operators by

$$G_C^{(c)}(Q^2) = \sqrt{\frac{4\pi E_{d'}^{(c)}E_d^{(c)}}{3M_d^2}}\frac{1}{1 + \eta}\frac{|\vec{q}_{lab}|}{|\vec{q}_c|}\langle 1\|C_0(Q^2)\|1\rangle^{(c)}\,, \tag{13}$$

$$G_Q^{(c)}(Q^2) = \sqrt{\frac{3\pi E_{d'}^{(c)}E_d^{(c)}}{2M_d^2}}\frac{1}{\eta(1 + \eta)}\frac{|\vec{q}_{lab}|}{|\vec{q}_c|}\langle 1\|C_2(Q^2)\|1\rangle^{(c)}\,, \tag{14}$$

$$G_M^{(c)}(Q^2) = -\sqrt{\frac{\pi E_{d'}^{(c)}E_d^{(c)}}{M_d^2}}\frac{i}{\sqrt{\eta(1 + \eta)}}\langle 1\|M_1(Q^2)\|1\rangle^{(c)}\,, \tag{15}$$

where we have introduced the notation $M_1(Q^2)$ instead of $T_1^{(m)}(Q^2)$ for the magnetic dipole operator. Then one finds for the longitudinal and transverse structure functions the well known expressions

$$W_L^{(c)}(Q^2) = (1+\eta)^2 \frac{\vec{q}_c^2}{\vec{q}_{lab}^2} \left(G_C^{(c)}(Q^2)^2 + \frac{8}{9}\eta^2 G_Q^{(c)}(Q^2)^2 \right), \tag{16}$$

$$W_T^{(c)}(Q^2) = \frac{4}{3}\eta(1+\eta)G_M^{(c)}(Q^2)^2. \tag{17}$$

The various multipole operators are evaluated between intrinsic deuteron wave functions in the chosen frame of reference "c".

With respect to the interpretation of the form factors, the following remark is in order. Since in the Breit frame one has the relation $Q^2 = (\vec{q}_{Breit})^2$, one usually interprets $G_C^{(Breit)}(Q^2)$ as the Fourier transform of the charge density of the target. However, this interpretation is misleading, since each Fourier component refers to a different reference frame, because the Breit frame depends on the momentum transfer. Indeed, C_0 in (13) contains according to (11) the effect of the boost of initial and final target states to its rest frame. In other words, the Fourier inversion of the form factor $G_C^{(Breit)}(Q^2)$ will not result in the rest frame charge density of the target, because the latter does not contain the boost effects.

In principle, the superscript "(c)" at the form factors is redundant because the form factors themselves are invariant quantities, independent from the chosen reference frame if they are evaluated in a genuine covariant theory. However, in a nonrelativistic or semirelativistic treatment, where only lowest order relativistic contributions are included, they will in general be frame dependent, and for this reason we have kept the superscript "(c)" on them. In fact, it would be quite instructive to study the frame dependence in such a case. For electrodisintegration this has been done in [19]. There we had introduced a so-called ζ-frame allowing a continuous variation of the reference frame between lab and antilab systems by variation of a parameter ζ between zero and one which corresponds to the antilab and lab frames, respectively. The Breit frame is described by $\zeta = 1/2$.

In the ζ-frame one has the following kinematic relations

$$\vec{d}_\zeta = -(1-\zeta)\vec{q}_\zeta, \quad E_{d_\zeta} = M_d \frac{1+2\eta(1-\zeta)}{\sqrt{1+4\eta\zeta(1-\zeta)}},$$
$$\vec{d}'_\zeta = \zeta\vec{q}_\zeta, \qquad E_{d'_\zeta} = M_d \frac{1+2\eta\zeta}{\sqrt{1+4\eta\zeta(1-\zeta)}}, \tag{18}$$

with

$$\vec{q}_\zeta = \frac{\vec{q}_{lab}}{\sqrt{1+4\eta\zeta(1-\zeta)}}. \tag{19}$$

Thus in the ζ-frame the form factors become

$$G_C^{(\zeta)}(Q^2) = \sqrt{\frac{4\pi}{3}} \frac{c_\zeta(\eta)}{1+\eta} \langle 1\|C_0(Q^2)\|1\rangle^{(\zeta)}, \tag{20}$$

$$G_Q^{(\zeta)}(Q^2) = \sqrt{\frac{3\pi}{2}} \frac{c_\zeta(\eta)}{\eta(1+\eta)} \langle 1\|C_2(Q^2)\|1\rangle^{(\zeta)}, \tag{21}$$

$$G_M^{(\zeta)}(Q^2) = -i\sqrt{\frac{\pi}{\eta(1+\eta)}} \frac{c_\zeta(\eta)}{\sqrt{1+4\eta\zeta(1-\zeta)}} \langle 1\|M_1(Q^2)\|1\rangle^{(\zeta)}, \tag{22}$$

where

$$\begin{aligned} c_\zeta(\eta) &= \sqrt{\frac{E_d E_{d'}}{M_d^2}} \frac{|\vec{q}_{lab}|}{|\vec{q}_\zeta|} \\ &= \sqrt{(1+2\eta(1-\zeta))(1+2\eta\zeta)} \\ &= \sqrt{1+2\eta+4\eta^2\zeta(1-\zeta)} \end{aligned} \tag{23}$$

takes into account the noncovariant normalization and the boost from the ζ- to the lab frame. These expressions are symmetric with respect to the interchange $\zeta \leftrightarrow (1-\zeta)$ which reflects the fact, that the ζ-frame is equivalent to the $(1-\zeta)$-frame. In particular, this means that lab and antilab frames are equivalent as has been noted before [20]. Thus for a check of the frame dependence one needs to consider only either ζ between 0 and 1/2 or between 1/2 and one.

In the lab or antilab frames one has $c_0(\eta) = c_1(\eta) = \sqrt{1+2\eta}$ and thus

$$G_C^{(lab/antilab)}(Q^2) = \sqrt{\frac{4\pi}{3}} \frac{\sqrt{1+2\eta}}{1+\eta} \langle 1\|C_0(Q^2)\|1\rangle^{(lab/antilab)}, \tag{24}$$

$$G_Q^{(lab/antilab)}(Q^2) = \sqrt{\frac{3\pi}{2}} \frac{\sqrt{1+2\eta}}{\eta(1+\eta)} \langle 1\|C_2(Q^2)\|1\rangle^{(lab/antilab)}, \tag{25}$$

$$G_M^{(lab/antilab)}(Q^2) = -i\sqrt{\frac{\pi(1+2\eta)}{\eta(1+\eta)}} \langle 1\|M_1(Q^2)\|1\rangle^{(lab/antilab)}, \tag{26}$$

whereas in the Breit frame with $c_{\frac{1}{2}}(\eta) = 1 + \eta$ one finds

$$G_C^{(Breit)}(Q^2) = \sqrt{\frac{4\pi}{3}} \langle 1\|C_0(Q^2)\|1\rangle^{(Breit)}, \tag{27}$$

$$G_Q^{(Breit)}(Q^2) = \sqrt{\frac{3\pi}{2}} \frac{1}{\eta} \langle 1\|C_2(Q^2)\|1\rangle^{(Breit)}, \tag{28}$$

$$G_M^{(Breit)}(Q^2) = -i\sqrt{\frac{\pi}{\eta}} \langle 1\|M_1(Q^2)\|1\rangle^{(Breit)}. \tag{29}$$

In the present work, however, we will adopt the antilab frame for the numerical evaluation.

The form factors are normalized as

$$G_C(0) = 1, \tag{30}$$

$$G_Q(0) = M_d^2 \, Q_d, \tag{31}$$

$$G_M(0) = \frac{M_d}{M_p} \, \mu_d, \tag{32}$$

where μ_d (in units of nuclear magnetons μ_N) and Q_d denote the static deuteron magnetic dipole and charge quadrupole moments, respectively, and M_p the proton mass. Furthermore, the mean square charge radius r_d^{ch} of the deuteron is defined by

$$(r_d^{ch})^2 = -6 \left. \frac{dG_C(Q^2)}{dQ^2} \right|_{Q^2=0}. \tag{33}$$

In the Breit frame it is usually interpreted as the mean square radius of the charge density (see Eq. (27)). One should keep in mind that r_d^{ch} includes the effect of finite nucleon and meson sizes.

Instead of the representation of the differential cross section in terms of the structure functions $W_{L/T}$ one usually introduces two other invariant structure functions $A(Q^2)$ and $B(Q^2)$ by defining

$$A(Q^2) = (1+\eta)^{-2} \frac{\vec{q}_{lab}^2}{\vec{q}_c^2} W_L^{(c)}(Q^2) + \frac{1}{2}(1+\eta)^{-1} W_T^{(c)}(Q^2)$$
$$= G_C^{(c)}(Q^2)^2 + \frac{8}{9}\eta^2 G_Q^{(c)}(Q^2)^2 + \frac{2}{3}\eta \, G_M^{(c)}(Q^2)^2 \tag{34}$$

$$B(Q^2) = W_T^{(c)}(Q^2)$$
$$= \frac{4}{3}\eta(1+\eta) \, G_M^{(c)}(Q^2)^2, \tag{35}$$

and the cross section becomes

$$\frac{d\sigma^{lab}}{d\Omega_e^{lab}} = \sigma_{Mott}^{lab} \left[A(Q^2) + B(Q^2) \tan^2 \frac{\theta_e^{lab}}{2} \right]. \tag{36}$$

A polarization observable of considerable interest is the tensor recoil polarization T_{20} because it is sensitive to the quadrupole form factor [21–23] according to

$$T_{20}(Q^2, \theta_e^{lab}) = -\frac{4\sqrt{2}\,\eta}{3S(Q^2, \theta_e^{lab})} \left(G_C(Q^2) \, G_Q^{(c)}(Q^2) + \frac{\eta}{3} G_Q^{(c)}(Q^2)^2 \right.$$
$$\left. + \frac{1}{8}\left(1 + 2(1+\eta)\tan^2 \frac{\theta_e^{lab}}{2}\right) G_M^{(c)}(Q^2)^2 \right), \tag{37}$$

5

where

$$S(Q^2, \theta) = A(Q^2) + B(Q^2) \tan^2 \frac{\theta}{2}. \tag{38}$$

Thus the measurement of T_{20} in conjunction with the structure functions $A(Q^2)$ and $B(Q^2)$ allows one to disentangle the charge monopole and quadrupole form factors.

III. RESULTS AND DISCUSSION

The various current contributions including relativistic terms of leading order beyond the nonrelativistic theory to one- and two-body charge and current density operators have been evaluated for the elastic form factors, the structure functions and the tensor polarization T_{20}. We have limited our evaluation to the region of momentum transfers $Q^2 \leq 30$ fm^{-2}, the reason being that in a previous study of electrodisintegration the limit of the nonrelativistic approach plus leading order relativistic contributions had been found to be roughly $Q^2 \sim 25$ fm^{-2} [19]. Therefore, results for higher momentum transfers obtained within such a limited framework may not be reliable, and there any agreement with experimental data may be accidental and misleading.

Our theoretical approach is based on the equation-of-motion method, and has been outlined in detail in [24]. Starting from a system of coupled nucleon and meson fields, one eliminates the explicit meson degrees of freedom by the FST-method [25] and introduces instead effective operators in pure nucleonic space for both the NN interaction and the electromagnetic charge and current densities. By means of the Foldy-Wouthuysen transformation, one obtains the nonrelativistic reduction including leading order relativistic contributions. Whereas in [24] only pion degrees of freedom have been considered, the extension to the three realistic Bonn OBEPQ versions A, B, and C [4] with application to electrodisintegration has been reported in [1]. All the relevant details can be found there. In particular, all explicit expressions are listed in the Appendix of [1] for the various one- and two-body contributions to the electromagnetic charge and current density operators used in this work, including consistently leading order relativistic terms, boost and vertex parts, and, furthermore, the lowest order dissociation $\rho\pi\gamma$-current, which is purely transverse and not fixed by the potential model. If not mentioned explicitly, the potental version OBEPQ-B is used. Each version fixes the masses, coupling strengths, and vertex regularization parameters for the various exchanged mesons. As electromagnetic nucleon form factors, we have taken the phenomenological dipole fit including a nonvanishing electric neutron form factor in the Galster parametrization [27]. For the following discussion of the effects from the various relativistic contributions, we use the same notational scheme as introduced in [1] which we list for convenience in Table I.

We will start the discussion by considering first the static electromagnetic properties, viz., magnetic dipole and electric quadrupole moments μ_d and Q_d, respectively, and the mean square charge radius r_d^{ch}. In Table II the various current contributions are listed for the OBEPQ-B model. Relativistic one-body contributions reduce slightly the magnetic moment of the nonrelativistic impulse approximation (IA) by 0.7 %, in good agreement with [14]. The same magnitude but of opposite sign has been found in [31] using a covariant light-front approach and a p/M-expansion as well. The reason for this difference is not clear to us. Relativistic pion exchange currents including boost then lead to an enhancement by about 1.8 % which, however, is again weakly reduced by retardation (-0.6 %). Further contributions of 1.7 % from ρ-exchange, of 0.8 % from other heavy mesons and of 0.5 % from the $\rho\pi\gamma$-current result in a total increase over the IA by 4.2 %. This is considerably larger than the 2.6 % which has been found in [16] with the Argonne potential v_{18}. It is also larger than the results found in [14]. Comparing with the individual contributions of [14], we find the only sizeable difference in the ones of π- and ρ-MEC, for which we obtain a total contribution which is larger by about a factor of two. The total theoretical magnetic moment of $0.8875 \, \mu_N$ is by 3.5 % higher than the experimental value of $0.8574 \, \mu_N$ [28].

The quadrupole moment is mainly affected by contributions from the pion exchange charge contribution giving a sizeable increase (4.9 %) while relativistic one-body (-0.7 %) and pion retardation (-0.4 %) contributions yield a smaller decrease. The relativistic one-body part is in agreement with the results of [14,15]. With respect to the total pion contribution we notice a nice agreement with [15] but again our result is considerably larger than what has been found in [14]. Heavy meson exchange is almost negligible. The total effect is an enhancement by 3.8 % over the IA, twice as large than found in [14] and [16], and the total theoretical value is in satisfactory agreement with the experimental value of $Q_d^{exp} = 0.2860(15) \, \text{fm}^2$ [29]. Finally, comparing the one-body part with the findings of [31], one notices again the puzzling situation that the relativistic one-body contributions lead to an enhancement in the covariant approach while the p/M-expansion results in a small decrease. Whether this hints at a failure of the p/M-expansion as interpreted in [31] needs further studies.

The charge radius is much less sensitive to relativistic and meson exchange contributions due to the suppression of the short range part by the additional r^2-weighting. We find a total enhancement of only 0.5 %, mainly from

relativistic one-body and pion exchange terms, all other effects being negligible here. The relativistic one-body part is somewhat smaller than reported in [32] while the MEC part is of the same size than found in [14] and [32] but slightly larger than in [33]. The total theoretical value of 2.1121 fm is in excellent agreement with the earlier experimental value of 2.116(6) from [30] and still quite close to the recent experimental one of 2.127(7) fm, the difference being only about 1 %. The latter value is based on an isotope shift experiment [34] resulting in $r_{IS}^2 = (r_d^{ch})^2 - (r_p^{ch})^2 = 3.795(19)$ fm^2 including first order nuclear structure effects. If one includes in addition second order nuclear structure effects from [35] one finds $r_{IS}^2 = (r_d^{ch})^2 - (r_p^{ch})^2 = 3.782(21)$ fm^2 as cited in a review by Wong [36]. We have taken the latter value and for the proton $r_p^{ch} = 0.862(12)$ fm from [30] to evaluate the experimental deuteron charge radius listed in Tables II and III.

The potential model dependence of the static e.m. deuteron properties is shown in Table III. The largest relative variation is found for the quadrupole moment of about 1.2 % increase going from model A to B and to C which is correlated with the increase of the tensor force as is indicated by the D-state percentage P_d listed also in Table III. Similarly, one finds a steady increase of the magnetic moment with increasing P_d, each time of about 0.5 % going from model A and B to C. Only the charge radius is almost independent from the potential model.

As next we will discuss the results for the form factors. The influence of various contributions are shown in Fig. 1 for the charge and quadrupole form factors and in Fig. 2 for the magnetic dipole form factor. In the left panels we show separately the effects of the relativistic one-body currents, of the one-body boost, and of the relativistic π-MEC. The additional effects from retardation and two-body boost for the π-MEC, from heavy meson exchange and from the $\rho\pi\gamma$-current are exhibited separately in the right panels. Looking first at the upper left panel of Fig. 1, one readily notices that the relativistic one-body contributions to the charge density show only a very tiny effect on $G_C(Q^2)$ while the corresponding one-body boost results in quite an enhancement and a sizeable shift of the zero towards higher momentum transfer. The significance of the one-body boost has already been observed before in [14,15] and and our results are in qualitative agreement with those findings. We would like to emphasize that neglect of this boost part as in the calculations of [13,16] leads to a significant overestimation.

Adding now the relativistic π-MEC, yields a strong reduction. In fact, it is by far the largest effect which reverses the upshift of the zero by relativistic one-body contributions and shifts it down beyond the nonrelativistic one. This important effect of the π-MEC is in accordance with earlier findings in, e.g., [11,13,16,37] and in particular with [17] and [18]. All other additional contributions, as shown in the upper right panel of Fig. 1, from π-retardation, two-body boost, heavy meson exchange are very small in this region of Q^2. The $\rho\pi\gamma$-current does not contribute, because we have considered its lowest order contribution only which is purely transverse. The situation for $G_Q(Q^2)$ in the lower left panel of Fig. 1 is different with respect to the relative importance of the various contributions. Here all relativistic one-body terms show much less effects compared to $G_C(Q^2)$, only π-MEC gives a sizeable increase of the form factor in accordance with the results in [17]. Again all other further contributions have an almost negligible influence on G_Q, as is seen in the lower right panel of Fig. 1.

For the magnetic dipole form factor $G_M(Q^2)$ the role of the various contributions is markedly different as can be seen in Fig. 2. In the left panel one notices that already the relativistic one-body currents lead to a significant decrease of the nonrelativistic IA. However, the one-body boost contributions are sizeable too, but act in the opposite direction so that the total result is very close to the original IA. Again the remark is in order that leaving out the one-body boost contributions leads to an underestimation. The inclusion of the relativistic π-MEC yields then a drastic increase with increasing momentum transfer. Adding retardation and boost for π-exchange, shown in the right panel, results in a slight reduction which is more than compensated by ρ-MEC. Further slight increases come from the additional contributions of other heavy meson exchanges and from the dissociation $\rho\pi\gamma$-current.

The observables, i.e., the structure functions $A(Q^2)$ and $B(Q^2)$, and the tensor polarization $T_{20}(Q^2, 70°)$ are displayed in Fig. 3, again with separate contributions shown in the left and right panels as for the form factors in the previous figures. For $A(Q^2)$, shown in the upper left panel, the relativistic one-body current gives a lowering of the IA above $Q^2 \sim 10$ fm^{-2}, which is counteracted by the corresponding boost terms so that the net result is only a tiny enhancement of the IA. A stronger increase is generated by the relativistic π-MEC, again above $Q^2 \sim 10$ fm^{-2}. All other additional contributions from retardation, two-body boost, heavy meson exchange and $\rho\pi\gamma$-current, shown in the upper right panel, are very small. Compared to the experimental data, also displayed in Fig. 3, one notices a satisfactory agreement for momentum transfers $Q^2 \leq 10$ fm^{-2}. For higher Q^2 the IA including relativistic one-body contributions lies systematically below the data, while addition of relativistic π-MEC results in a systematic overshooting which is not compensated enough by the slight reduction from the heavy meson and $\rho\pi\gamma$-currents. This overshooting has also been observed in [18].

The behaviour of $B(Q^2)$, shown in the middle left and right panels, reflects the one of $G_M(Q^2)$ in Fig. 2 and thus we do not need to discuss the various relativistic contributions again in detail. With respect to experiment, already at rather low momentum transfers, the IA plus relativistic one-body contributions lies below the experimental data. Here the inclusion of the relativistic π-MEC leads to quite a satisfactory agreement although the theory lies

systematically slightly higher than the data. It corresponds to what has been noted above for the static magnetic moment μ_d. However, the further contributions from the heavy meson and $\rho\pi\gamma$-currents spoil this nice agreement and lead to a sizeable overestimation, considerably larger than for $A(Q^2)$. Such a systematic overprediction has also been observed by Plessas *et al.* [18] as well as by Wiringa et al. [16] although in the latter case of somewhat smaller size, but they had left out the boost contributions which would have shifted further up their results. The origin of this systematic disagreement is an open question and it needs further detailed studies to clarify it. Obviously, it appears that the magnetic properties of hadronic systems are more sensitive to finer details of the dynamic interaction effects than charge ones, for which charge conservation constitutes a stringent condition. It is interesting to note that the recent relativistic calculation of Phillips *et al.* [7] results in a systematic underestimation of the data for both structure functions in this region of momentum transfers.

The two lower panels of Fig. 3 show the influence of the various current contributions on the tensor polarization $T_{20}(Q^2, 70°)$. Since the minimum is determined by the zero of $G_C(Q^2)$, one readily notices that the shift of the minimum by the different current contributions follows the shift of the zero of $G_C(Q^2)$, i.e., the largest effects come from the one-body boost shifting the minimum to higher Q^2 and from the π-exchange resulting in an even larger downshift of the minimum and of the zero crossing of $T_{20}(Q^2, 70°)$. With respect to the experimental data, the one-body currents alone yield a drastic disagreement for momentum transfers above the minimum, whereas inclusion of the relativistic π-MEC gives an almost satisfactory description although the data seem to rise slightly steeper at higher momentum transfers. All other further contributions show almost no influence at all.

Finally we show in Fig. 4 the dependence of form factors and observables on the three Bonn OBEPQ versions A, B, and C. The largest dependence on the potential model is seen in $G_C(Q^2)$ above $Q^2 \sim 10$ fm^{-2} via the shift of the zero. With increasing D-state probability P_d the zero is shifted downward. In contrast to this, $G_Q(Q^2)$ is rather insensitive to the potential model. This different behaviour is also reflected in the observables $A(Q^2)$ and $T_{20}(Q^2, 70°)$. The structure function $A(Q^2)$ in the upper right panel is almost model independent for $Q^2 \leq 10$ fm^{-2} while above this region some model dependence is seen which increases with increasing Q^2. Also the tensor polarization $T_{20}(Q^2, 70°)$ in the lower right panel exhibits very little model dependence up to $Q^2 \sim 10$ fm^{-2}, but at higher momentum transfers one notes a sizeable shift of the zero and a corresponding shift of the minimum towards higher Q^2 with increasing strength of the tensor force, i.e., increasing P_d, of the potential model. The magnetic form factor $G_M(Q^2)$ and thus $B(Q^2)$, shown in the middle left and right panels, respectively, exhibit an even larger sensitivity to the potential model over the whole region of momentum transfers which increases in size. The absolute values are correlated with the strength of the tensor force, i.e., one finds the highest values for the potential model C having the strongest tensor force.

We furthermore show in Fig. 4 a comparison with the experimental data for the observables. In order to exhibit more clearly the deviations between the three potential versions and from the experimental data we show in addition separately for the structure functions $A(Q^2)$ and $B(Q^2)$ in Fig. 5 the relative deviation with respect to the theoretical predictions of the OBEPQ-A model including all current contributions. As already stated, at low momentum transfers $(Q^2 \leq 10$ fm$^{-2})$ the potential model dependence of $A(Q^2)$ is negligible, and all potential models give a satisfactory agreement with the data. Above $Q^2 \sim 10$ fm^{-2}, however, increasing overestimation of the data is seen for $A(Q^2)$ for all three models, the largest deviation being for the OBEPQ-C model having the largest P_d, whereas for the OBEPQ-A model with the smallest P_d the theory is much closer to the data. For $B(Q^2)$ one notices already at low momentum transfers a systematic overestimation of the data by all three models in accordance with the overestimation of the static magnetic dipole moment. The deviation increases noticably with increasing momentum transfers. Again one readily sees a strong correlation between the size of the deviation and the size of P_d. As has been remarked already above with respect to the results with the potential model B, one finds for all three potential models a considerably larger overprediction for $B(Q^2)$ compared to $A(Q^2)$.

Within the experimental errors $T_{20}(Q^2, 70°)$ is well described by the predictions for the OBEPQ-B model, but also the results for the other two OBEPQ models are in reasonable agreement in view of the large error bars. The new data above 15 fm^{-2} from [49] seem to favour the OBEPQ-C model but one has to await the final data analysis before one could make such a definite conclusion. Considering all data, the best overall description is achieved with the OBEPQ-B model at present. But, as already mentioned, above $Q^2 \sim 15$ fm^2 the data seem to rise steeper. Thus a more precise location of the zero crossing would be most interesting.

In conclusion we may state that the consistent inclusion of all important relativistic contributions of leading order within a pure nucleonic one-boson-exchange model leads to a satisfactory description of the structure functions of elastic electron-deuteron scattering at low and medium momentum transfers $(Q^2 \leq 30$ fm$^2)$ for the OBEPQ-A model, if one satisfies oneself with an agreement between theory and experiment within the level of about ten to twenty percent for $A(Q^2)$, whereas for $B(Q^2)$ the deviation grows considerably larger, e.g., a factor two at $Q^2 = 25$ fm^2. The tensor polarization is better described with the OBEPQ-B model. If, however, one aimes at a more precise agreement at the level of one or even less than one percent, significant further improvements are needed, in particular a much better description for the magnetic properties will be a very challenging task for the future. One might speculate

whether explicit isobar [51–53] or even quark-gluon degrees of freedom [12] might lead to a significant improvement or whether other off-shell effects in electromagnetic form factors of the various currents may be important.

We would like to add another remark concerning the quality of the Bonn OBEPQ potentials, considered in this work, compared to more recent so-called "high quality" NN-potentials. These latter potentials use a slightly smaller πN-coupling constant than the one taken in the above OBEPQ potentials [54]. This affects in particular the strength of the tensor force becoming somewhat weaker in these modern NN-potentials which in turn would lead to a smaller quadrupole moment of the deuteron. A way out of this dilemma is discussed in [54] by assuming a charge splitting of the πN-coupling constant. Therefore, it remains as a task for the future to study these high quality potentials in elastic electron deuteron scattering. Due to the phenomenological character of these potentials, the construction of a consistent current is quite involved. Our results, however, underline the necessity of such a consistent calculation, since otherwise any conclusions drawn would be rather premature.

---

[1] F. Ritz, H. Göller, T. Wilbois, and H. Arenhövel, Phys. Rev. C **55**, 2214 (1997).
[2] F. Ritz, H. Arenhövel, and T. Wilbois, Few-Body Syst. **24**, 123 (1998).
[3] R. Machleidt, K. Holinde, and Ch. Elster, Phys. Rep. **149**, 1 (1987).
[4] R. Machleidt, Adv. Nucl. Phys. **19**, 189 (1989).
[5] F. Gross, in *Modern Topics in Electron Scattering*, eds. B. Frois and I. Sick (World Scientific, Singapore, 1991) p. 219.
[6] S.J. Wallace, Nucl. Phys. A **631**, 137c (1998).
[7] D.R. Phillips, S.J. Wallace, and N.K. Devine, nucl-th/9906086.
[8] M. Gourdin, *Diffusion des Électrons de Haute Énergie* (Masson, Paris, 1966).
[9] J.S. Levinger, Springer Tracts in Modern Physics, Vol. **71**, p. 88 (Springer-Verlag, Berlin, 1974).
[10] C. Ciofi degli Atti, Prog. Part. Nucl. Phys. **3**, 163 (1980).
[11] B. Mosconi and P. Ricci, Few-Body Syst. **6**, 63 (1989).
[12] A.J. Buchmann, Y. Yamauchi, and A. Faessler, Nucl. Phys. A **496**, 621 (1989).
[13] R. Schiavilla and D.O. Riska, Phys. Rev. C **43**, 437 (1991).
[14] K. Tamura, T. Niwa, T. Sato, and H. Ohtsubo, Nucl. Phys. **A536**, 597 (1992).
[15] J. Adam, Jr., H. Göller, and H. Arenhövel, Phys. Rev. C **48**, 370 (1993).
[16] R.B. Wiringa, V.G. Stoks, and R. Schiavilla, Phys. Rev. C **51**, 38 (1995).
[17] H. Henning, J. Adam, Jr., P.U. Sauer, and A. Stadler, Phys. Rev. C **52**, R471 (1995).
[18] W. Plessas, V. Christian, and R.F. Wagenbrunn, Few-Body Syst. Suppl. **9**, 429 (1995).
[19] G. Beck, T. Wilbois, and H. Arenhövel, Few-Body Syst. **17**, 91 (1994).
[20] K. Ohta, J. Phys. G **14**, 449 (1988).
[21] D. Schildknecht, Phys. Lett. **10**, 254 (1964); Z. Phys. **185**, 382 (1965).
[22] M. Gourdin and C.A. Piketty, Nuovo Cimento **32**, 1137 (1964).
[23] M.J. Moravcsik and P. Ghosh, Phys. Rev. Lett. **32**, 321 (1974).
[24] H. Göller and H. Arenhövel, Few-Body Syst. **13**, 117 (1992).
[25] N. Fukuda, K. Sawada, and M. Taketani, Progr. Theor. Phys. **12**, 156 (1954).
[26] J. Adam, Jr., E. Truhlik, and D. Adamova, Nucl. Phys. **A492**, 556 (1989).
[27] S. Galster, H. Klein, J. Moritz, K.H. Schmidt, D. Wegener, and J. Bleckwenn, Nucl. Phys. **B32**, 221 (1971).
[28] E.R. Cohen and B.N. Taylor, Rev. Mod. Phys. **59**, 1121 (1987).
[29] D.M. Bishop and L.M. Cheung, Phys. Rev. A **20**, 381 (1979); T.E.O. Ericson and M. Rosa-Clot, Nucl. Phys. **405**, 497 (1983).
[30] G.G. Simon, Ch. Schmitt, and V.H. Walther, Nucl. Phys. A **364**, 285 (1981).
[31] P.L. Chung, B.D. Keister, and F. Coester, Phys. Rev. C **39**, 1544 (1989).
[32] A.J. Buchmann, H. Henning, and P.U. Sauer, Few-Body Syst. **21**, 149 (1996).
[33] M. Kohno, J. Phys. G **9**, L85 (1983).
[34] F. Schmidt-Kaler, D. Leibfried, M. Weitz, and T.W. Hänsch, Phys. Rev. Lett. **70**, 2261 (1993).
[35] Y. Lu and R. Rosenfelder, Phys. Lett. B **319**, 7 (1993); Phys. Lett. B **333**, 564 (1994) (E).
[36] C.W. Wong, Int. J. Mod. Phys. E **3**, 821 (1994).
[37] M.I. Haftel, L. Mathelitsch, and H.F.K. Zingl, Phys. Rev. C **22**, 1285 (1980).
[38] J.E. Elias, J.L. Friedman, G.C. Hartmann, H.W. Kendall, P.N. Kirk, M.R. Sogard, L.P. Van Speybroeck, and J.K. de Pagter, Phys. Rev. **177**, 2075 (1969).
[39] R. Cramer *et al.*, Z. Phys. C **29**, 513 (1985).
[40] S. Auffret *et al.*, Phys. Rev. Lett. **54**, 649 (1985).

[41] S. Platchkov *et al.*, Nucl. Phys. A **510**, 740 (1990).
[42] M. Garçon *et al.*, Phys. Rev. C **49**, 2516 (1994).
[43] D. Abbott *et al.*, Phys. Rev. Lett. **82**, 1379 (1999).
[44] M.E. Schulze *et al.*, Phys. Rev. Lett. **52**, 597 (1984).
[45] V.F. Dmitriev *et al.*, Phys. Lett. **157B**, 143 (1985).
[46] R. Gilman *et al.*, Phys. Rev. Lett. **65**, 1733 (1990).
[47] I. The *et al.*, Phys. Rev. Lett. **67**, 173 (1991).
[48] M. Ferro-Luzzi *et al.*, Phys. Rev. Lett. **77**, 2630 (1996).
[49] C. Furget *et al.*, Acta Phys. Pol. B **29**, 3301 (1998).
[50] M. Bouwhuis *et al.*, Phys. Rev. Lett. **82**, 3755 (1999).
[51] W. Fabian, H. Arenhövel, and H.G. Miller, Z. Phys. **271**, 93(1974).
[52] H.J. Weber and H. Arenhövel, Phys. Rep. **36**, 279 (1978).
[53] P. Obersteiner, W. Plessas, and J. Pauschenwein, Few-Body Syst. Suppl. **5**, 140 (1992).
[54] R. Machleidt, nucl-th/9909036.

TABLE I.   Explanation of the notation used in the tables and figure captions.

notation	explanation
n	nonrelativistic nucleon current
$n(r)$	relativistic nucleon current
$n(r,\chi_0)$	relativistic nucleon current including kinematic boost currents
$\pi(r)$	static relativistic π-MEC
$\pi(r,t)$	$\pi(r)$ + retardation contributions
$\pi(r,t,\chi_0,\chi_V)$	$\pi(r,t)$ + kinematic and potential dependent boost currents
$\rho(\chi_0)$	full ρ-MEC + kinematic boost currents
$h(\chi_0)$	heavy meson exchange currents $(\eta,\omega,\sigma,\delta)$ + kinematic boost currents
d	$\rho\pi\gamma$-current
total	$n(r,\chi_0)\pi(r,t,\chi_0,\chi_V)\rho(\chi_0)h(\chi_0)d$

TABLE II. Static properties of the deuteron (magnetic dipole moment μ_d, electric quadrupole moment Q_d, and mean square charge radius r_d^{ch}) in various approximations for the Bonn OBEPQ-B model.

ingredient	$\mu_d\,[\mu_N]$	$Q_d\,[\mathrm{fm}^2]$	$r_d^{ch}\,[\mathrm{fm}]$
n	0.8515	0.2780	2.1016
$n(r,\chi_0)$	0.8457	0.2762	2.1073
$n(r,\chi_0)\pi(r)$	0.8673	0.2899	2.1120
$n(r,\chi_0)\pi(r,t,\chi_0,\chi_V)$	0.8624	0.2888	2.1122
$n(r,\chi_0)\pi(r,t,\chi_V)\rho(\chi_0)$	0.8767	0.2888	2.1122
$n(r,\chi_0)\pi(r,t,\chi_V)\rho(\chi_0)h(\chi_0)$	0.8833	0.2886	2.1121
total	0.8875	0.2886	2.1121
experiment	0.857438230(24) [28]	0.2860(15) [29]	2.116(6) [30]
			2.127(7)[a]

[a]from isotope shift experiment, for the reference see text.

TABLE III. Static properties of the deuteron (magnetic dipole moment μ_d, electric quadrupole moment Q_d, mean square charge radius r_d^{ch}) including all leading order relativistic contributions, and the D-wave percentage P_d for the various Bonn OBEPQ models.

potential model	$\mu_d\,[\mu_N]$	$Q_d\,[\mathrm{fm}^2]$	$r_d^{ch}\,[\mathrm{fm}]$	$P_d\,[\%]$
OBEPQ-A	0.8841	0.2850	2.1120	4.38
OBEPQ-B	0.8875	0.2886	2.1121	4.99
OBEPQ-C	0.8917	0.2917	2.1112	5.61
experiment	0.857438230(24) [28]	0.2860(15) [29]	2.116(6) [30]	
			2.127(7)[a]	

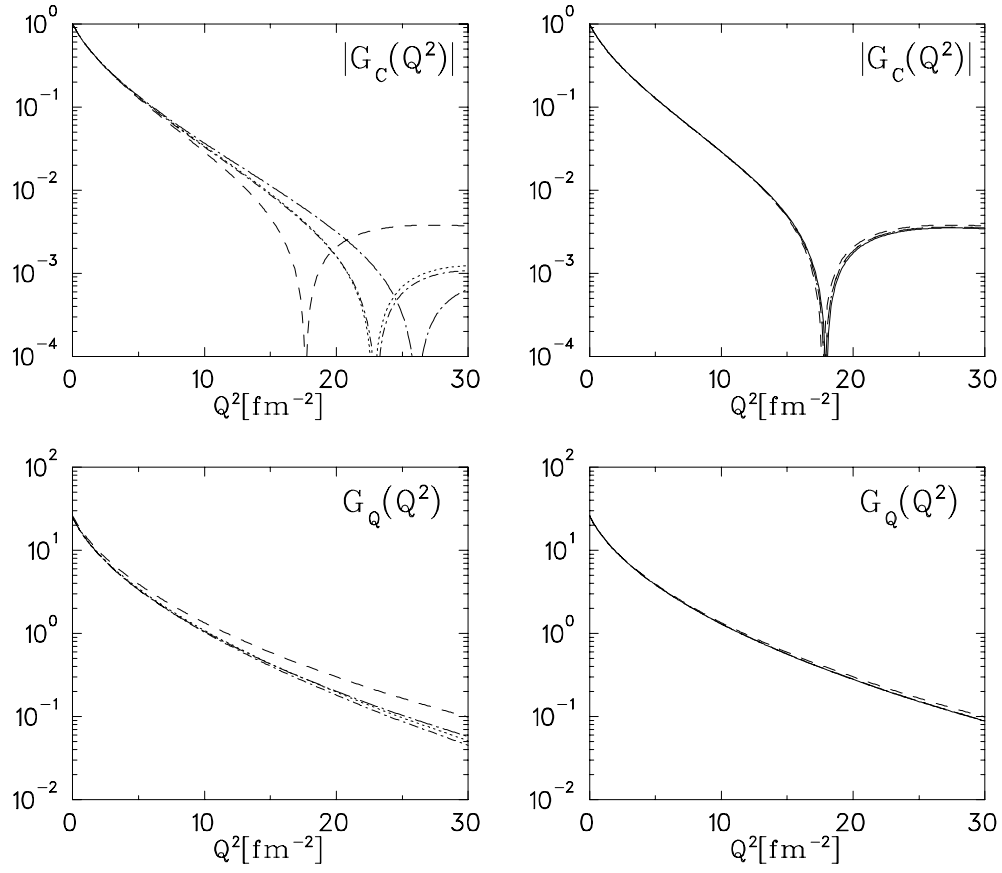[a]from isotope shift experiment, for the reference see text.

FIG. 1. Various current contributions to charge monopole and quadrupole form factors $G_C(Q^2)$ and $G_Q(Q^2)$, respectively, for the Bonn OBEPQ-B potential model as function of Q^2. Notation of the curves in the left panels: dotted: n; short-dash-dot: $n(r)$; long-dash-dot: $n(r, \chi_0)$; short dashed: $n(r, \chi_0)\pi(r)$; in the right panels: short dashed: $n(r, \chi_0)\pi(r)$; long dashed: $n(r, \chi_0)\pi(r, t)$; wide dotted: $n(r, \chi_0)\pi(r, t, \chi_0, \chi_V)$; solid: total.
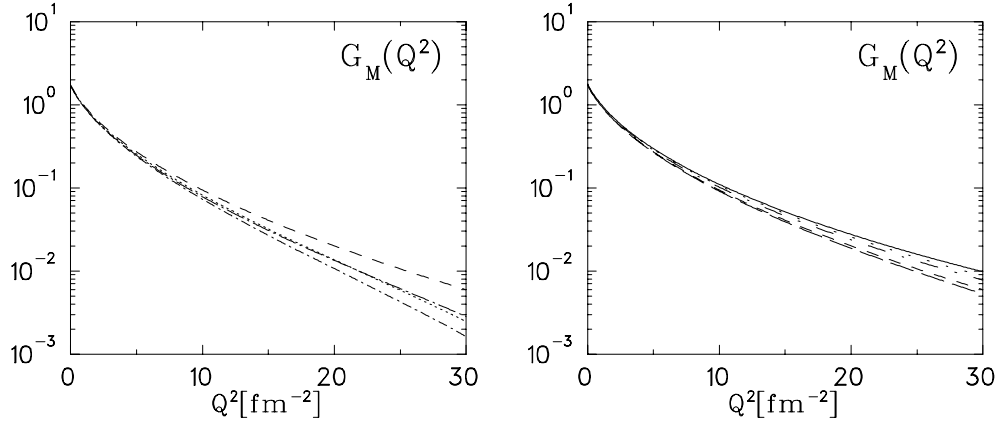
FIG. 2. Various current contributions to magnetic dipole form factor $G_M(Q^2)$ for the Bonn OBEPQ-B potential model as function of Q^2. Notation of the curves in the left panel: dotted: n; short-dash-dot: $n(r)$; long-dash-dot: $n(r, \chi_0)$; short dashed: $n(r, \chi_0)\pi(r)$; in the right panel: short dashed: $n(r, \chi_0)\pi(r)$; long dashed: $n(r, \chi_0)\pi(r, t, \chi_0, \chi_V)$; wide dash-dot: $n(r, \chi_0)\pi(r, t, \chi_0, \chi_V)\rho$; wide dotted: $n(r, \chi_0)\pi(r, t, \chi_0, \chi_V)\rho(\chi_0)h(\chi_0)$; solid: total.
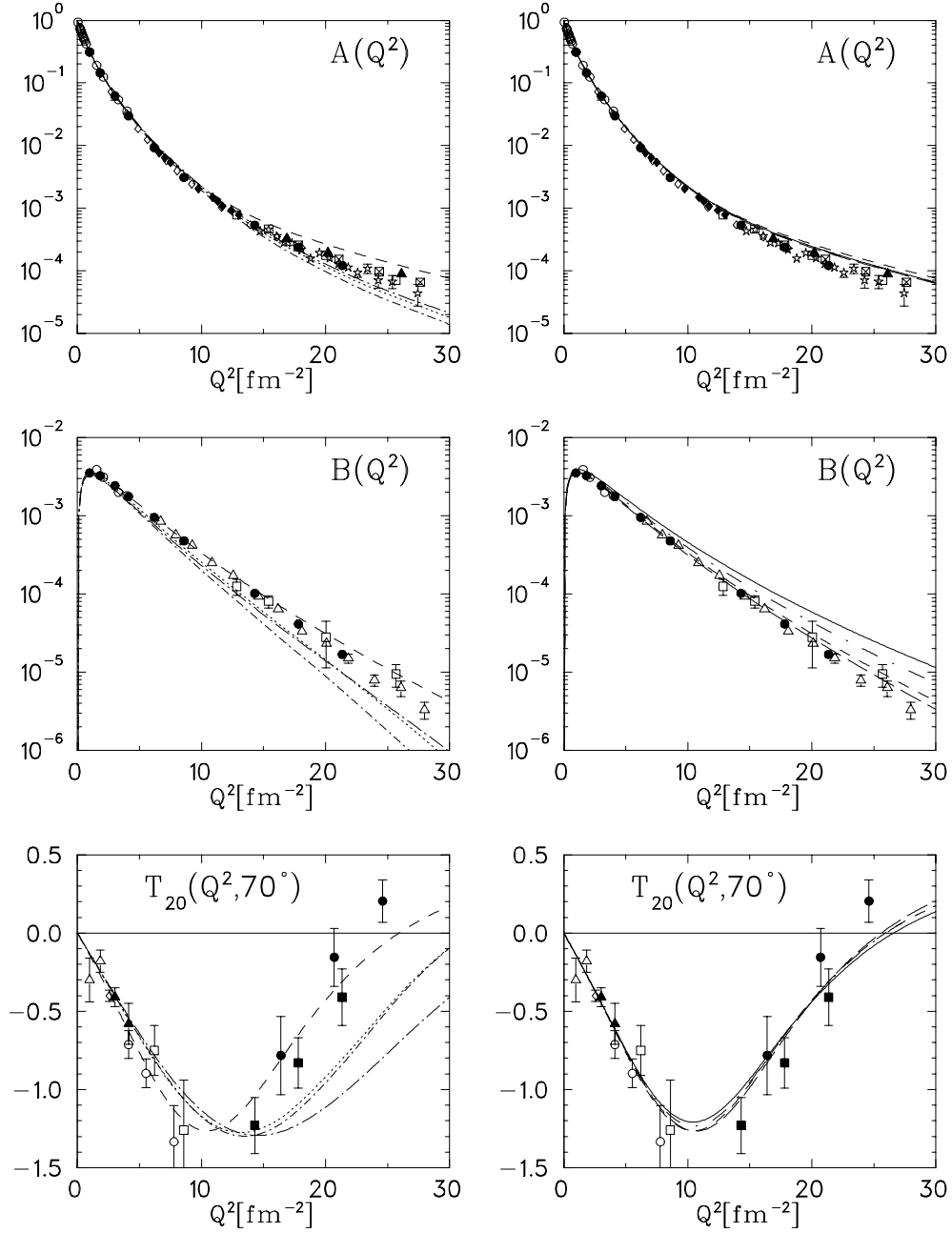
FIG. 3. Various current contributions to the structure functions $A(Q^2)$, $B(Q^2)$, and the tensor polarization $T_{20}(Q^2, 70°)$ for the Bonn OBEPQ-B potential model as function of Q^2. Notation of the curves in the left panels: dotted: n; short-dash-dot: $n(r)$; long-dash-dot: $n(r, \chi_0)$; short dashed: $n(r, \chi_0)\pi(r)$; in the right panels: short dashed: $n(r, \chi_0)\pi(r)$; long dashed: $n(r, \chi_0)\pi(r, t)$; wide dotted: $n(r, \chi_0)\pi(r, t, \chi_0, \chi_V)$; solid: total. Experimental data for $A(Q^2)$ and $B(Q^2)$: open stars: [38]; full diamonds: [27]; open circles: [30]; open squares: [39]; open triangles: [40]; open diamonds: [41]; full circles [42]; full triangles: [43]; Experimental data for $T_{20}(Q^2, 70°)$: full triangles: [44]; open triangles: [45]; open squares: [46]; full squares: [47]; open diamond: [48]; full circles: [49] (preliminary); open circles: [50].
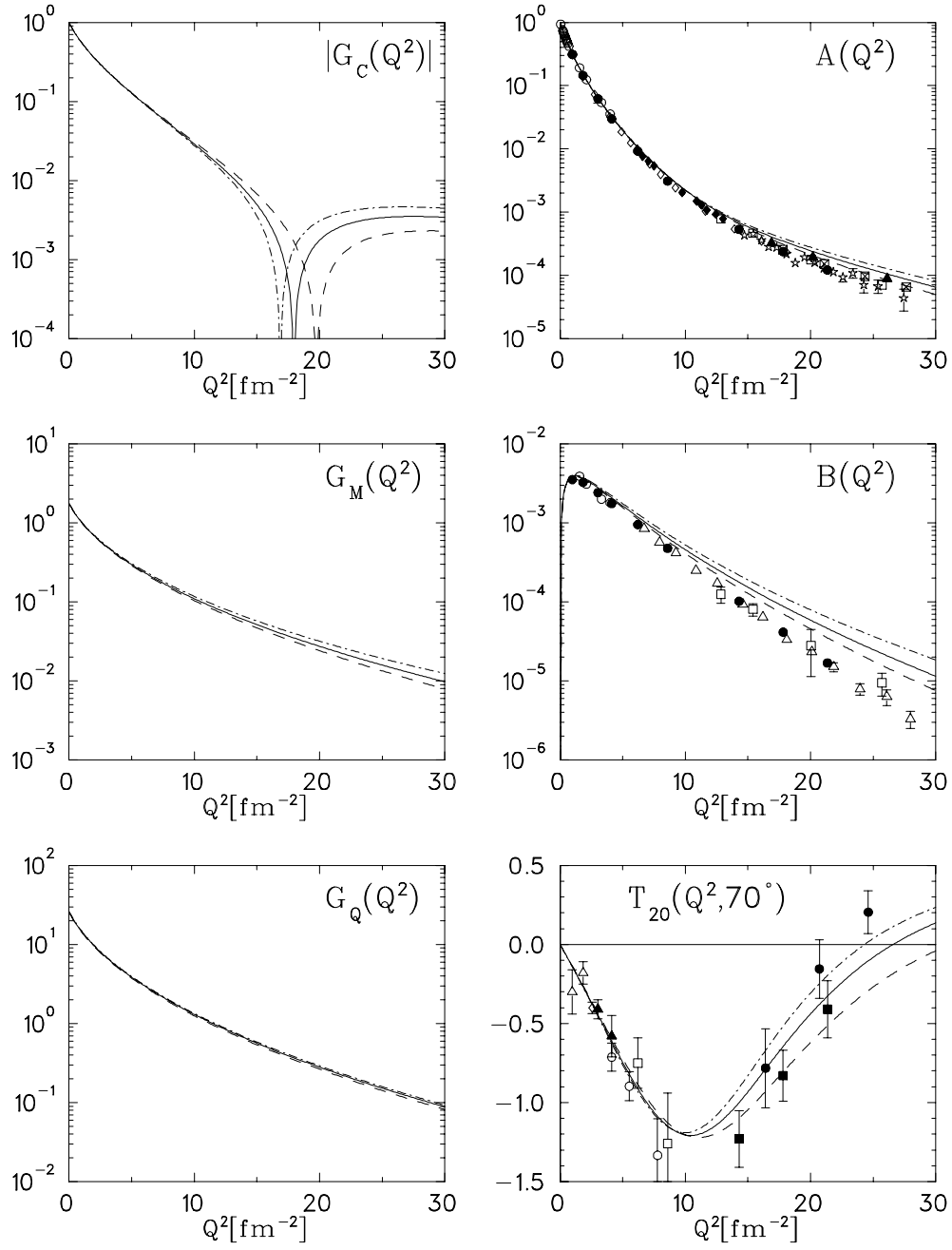
13

FIG. 4. Comparison of the three Bonn OBEPQ potential versions for the form factors and observables for the total current contributions. Notation of the curves: dashed: OBEPQ-A; solid: OBEPQ-B; dash-dot: OBEPQ-C. Experimental data as in Fig. 3.
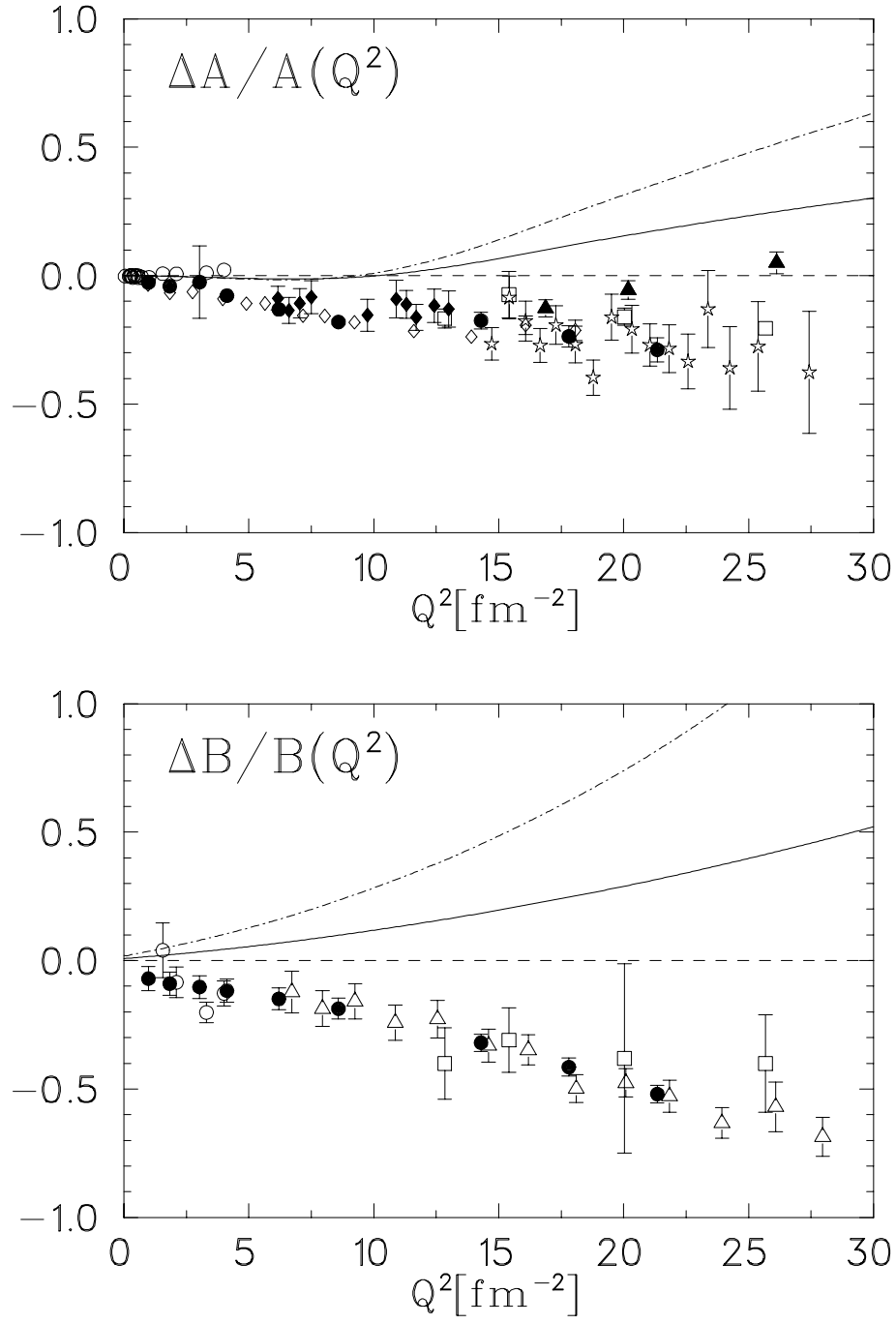
FIG. 5. Relative deviation of the structure functions $A(Q^2)$ and $B(Q^2)$ from the theoretical prediction for the Bonn OBEPQ-A potential including all current contributions. Notation of the curves: dashed: OBEPQ-A; solid: OBEPQ-B; dash-dot: OBEPQ-C. Experimental data as in Fig. 3.